Supporting Information

Optimal Coordination-Site Exposure Engineering in Porous Platinum for Outstanding Oxygen Reduction Performance

Han Cheng, [+a] *Si Liu*, [+a] *Zikai Hao*, [b] *Jingyu Wang*, [a] *Bojun Liu*, [a] *Guangyao Liu*, [a] *Xiaojun Wu*, [b] *Wangsheng Chu*, [c] *Changzheng Wu*, [a]* *and Yi Xie* [a]

[a] Hefei National Laboratory for Physical Sciences at the Microscale, iChEM (Collaborative Innovation Center of Chemistry for Energy Materials), CAS Key Laboratory of Mechanical Behavior and Design of Materials, University of Science and Technology of China, Hefei, Anhui 230026 P. R. China;

[b] CAS Key Laboratory of Materials for Energy Conversion and Department of Material Science and Engineering, University of Science and Technology of China, Hefei, Anhui 230026 (P. R. China)

[c] National Synchrotron Radiation Laboratory, University of Science and Technology of China Hefei, Anhui 230029, P. R. China;

* Correspondence and requests for materials should be addressed to C. Z. Wu (email: czwu@ustc.edu.cn)

[+] These authors contributed equally to this work.

S1. The RRDE measurement for GBP-Pt-600

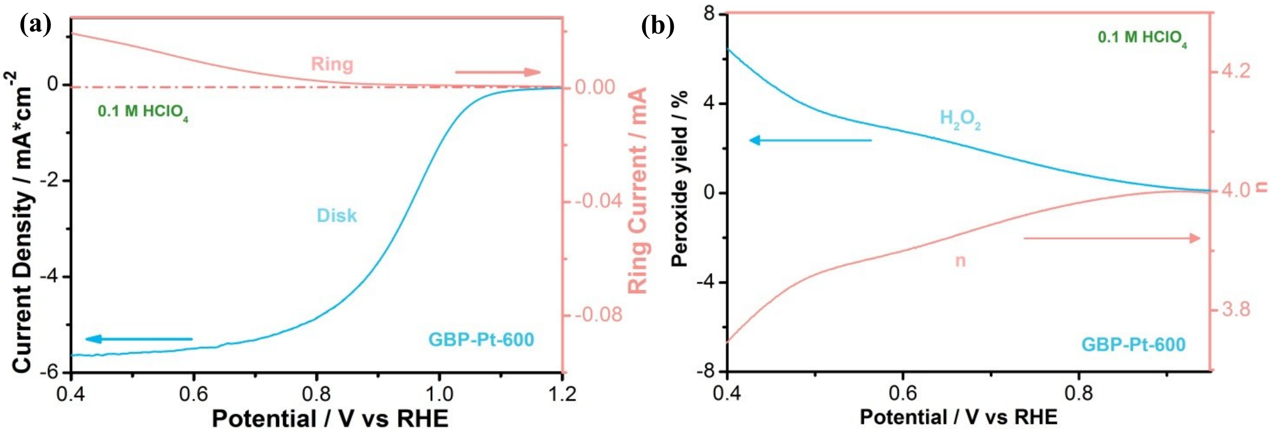

Figure S1. (a) The RRDE measurement for GBP-Pt-600. (b) Corresponding the peroxide yield and n value for GBP-Pt-600.

The rotating ring-disk electrode (RRDE) measurements were also tested in same catalysts' loading. A glassy carbon (GC, f=5.61 mm) disk-Pt ring RRDE was used. To determine H_2O_2 yield, the ring electrode was held at 1.30 V to oxidize H_2O_2 diffused from disk electrode. The Hydrogen peroxide yield (%H_2O_2) and the electron transfer number (n) were calculated by the followed equations:

$$\%H_2O_2 = 200\frac{i_r/N}{i_d + i_r/N} \quad (1)$$

$$n = 4\frac{i_d}{i_d + i_r/N} \quad (2)$$

Where i_d and i_r are the disk and ring currents, respectively. N is the ring current collection efficiency which was determined to be 37%.

S2. Hydrogen under potential deposition (HUPD) charge

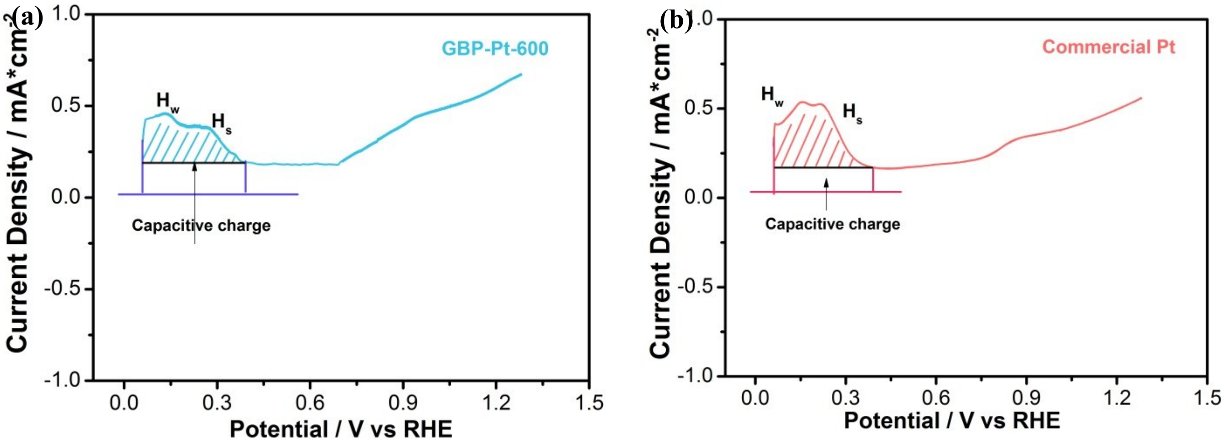

Figure S2. (a) Hydrogen under potential deposition charge for GBP-Pt-600 and (b) commercial Pt. Scan rate: 20 mV S^{-1}; catalyst loading: 20 $\mu g_{Pt}/cm^2$.

The stripping charge under the cyclic voltammetry (CV) between 0.05 and 0.4 V/RHE was corrected for capacitive contributions (0.4-0.55V background subtraction) and normalized with the theoretical charge per unit area $Q_{\text{theo, Pt}} = 210\ \mu C\ cm^{-2}$. The calculated electrochemical surface area (ECSA) for GBP-Pt-600 is 40.7 $m^2\ g^{-1}$ and for commercial Pt is 58.2 $m^2\ g^{-1}$.

S3. Cyclic stability test for commercial Pt

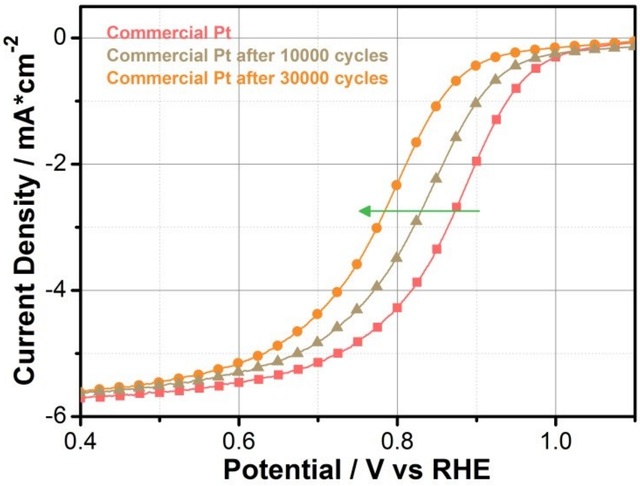

Figure S3. (a) Cyclic stability test for commercial Pt at BOL, after 10000 cycles and 30000 cycles.

S4. Pt L_3-edge EXAFS fitted in the r space by the IFEFFIT code

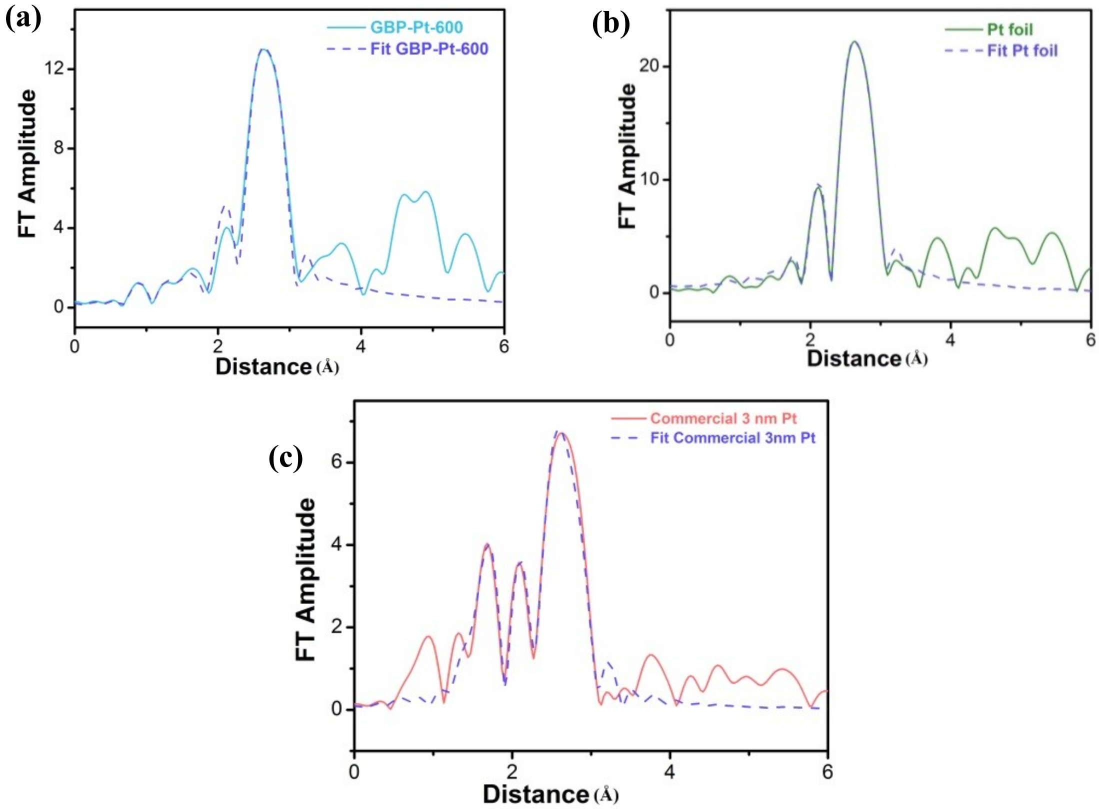

Figure S4 The Pt L_3-edge EXAFS fitted in the r space by the IFEFFIT code. (a) GBP-Pt-600 sample and fitted curves. (b) Pt foil sample and fitted curves. (c) Commercial Pt sample and fitted curves.

S5. The HAADF-STEM images of GBP-Pt-600

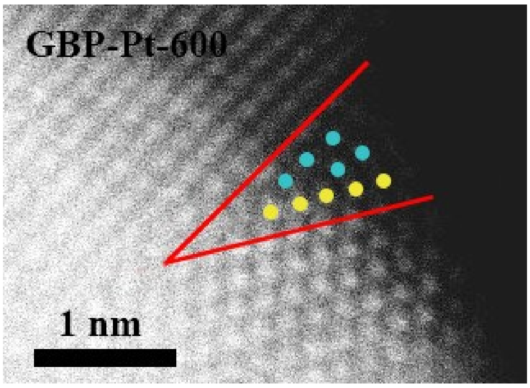

Figure S5. The high-angle annular dark-field scanning transmission electron microscopy (HAADF-STEM) of GBP-Pt-600.

S6. The ex-situ XAFS data for GBP-Pt-600 after fuel cell

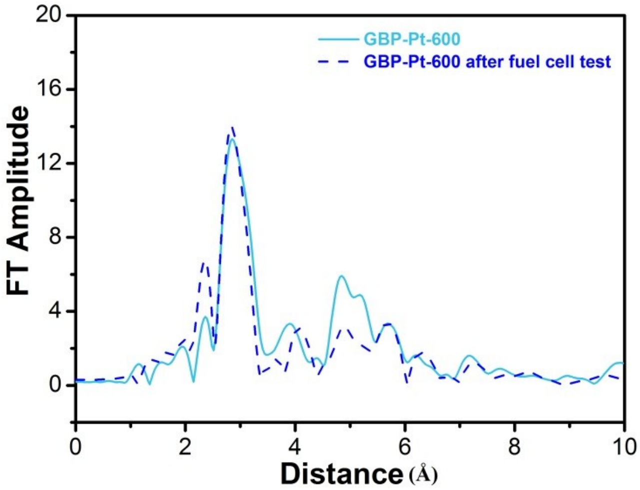

Figure S6. The ex-situ XAFS data for GBP-Pt-600 after fuel cell.

S7. The TEM images of GBP-Pt-600

(a) (b)

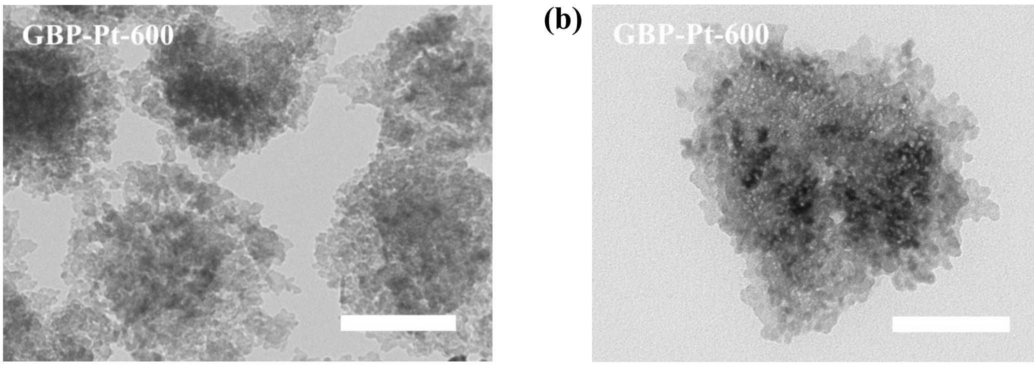

Figure S7. The transmission electron microscopy images of GBP-Pt-600. The scale bar is 50 nm (a) and 20 nm (b).

S8. The HRTEM images and SAED of GBP-Pt-600

(a)

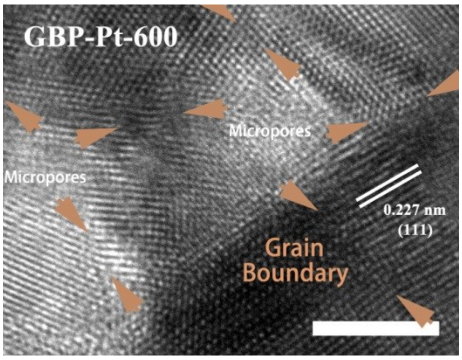

(b)

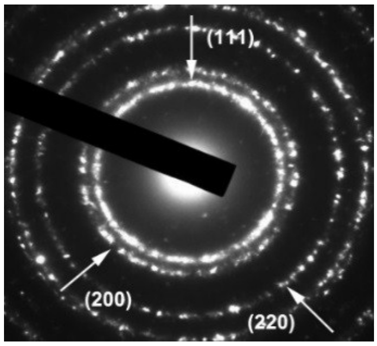

Figure S8. (a) The HRTEM images and SAED of GBP-Pt-600. The scale bar is 2 nm. (b) Selected area electron diffraction SAED images of the GBP-Pt-600.

S9. The XRD patterns of the Pt-CN precursors and GBP-Pt-600

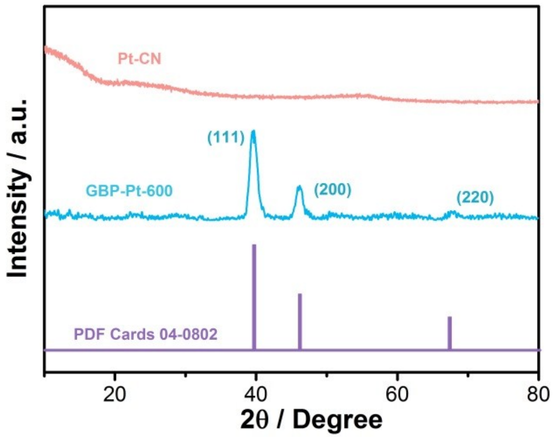

Figure S9. The XRD patterns of the Pt-CN precursors and GBP-Pt-600.

S10. The HRTEM images of the Pt-CN precursors

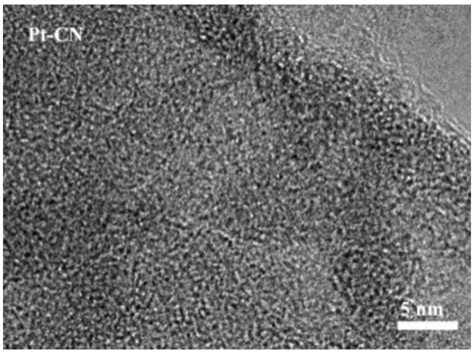

Figure S10. High resolution TEM images of the Pt-CN precursors.

S11. The STEM-EDX images of the Pt-CN precursors

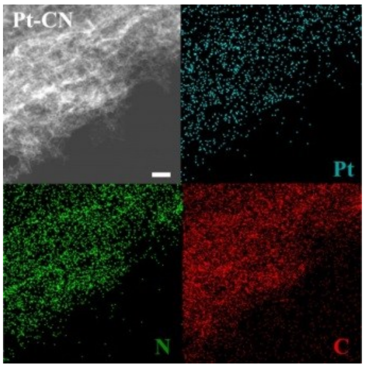

Figure S11. High-scanning TEM energy dispersive X-ray spectroscopic (STEM-EDX) of the Pt-CN precursors. The scale bar is 10 nm.

S12. The XPS spectra of the Pt-CN precursors and GBP-Pt-600

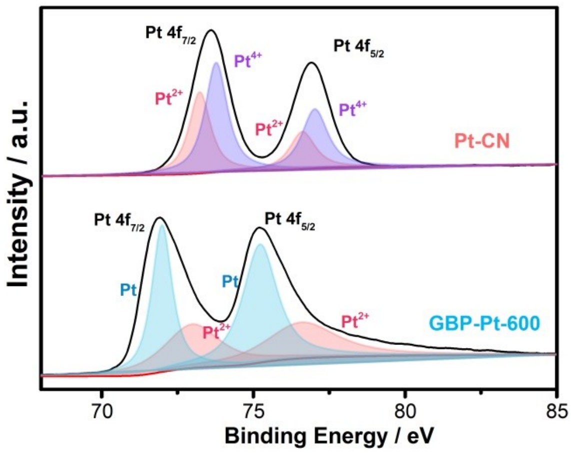

Figure S12. The XPS spectra of the Pt-CN precursors and GBP-Pt-600.

S13. The EELS of GBP-Pt-600

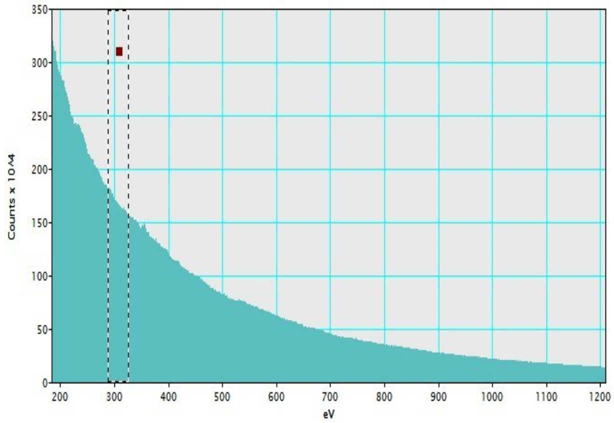

Figure S13. Electron Energy Loss Spectroscopy of the GBP-Pt-600.

S14. The TGA test for growth mechanism

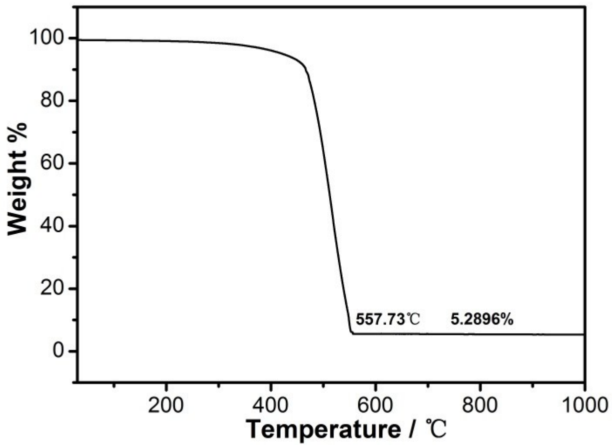

Figure S14. The TGA test from Pt-CN to GBP-Pt-600.

S15. The HRTEM images for GBP-Pt-600 after fuel cell test

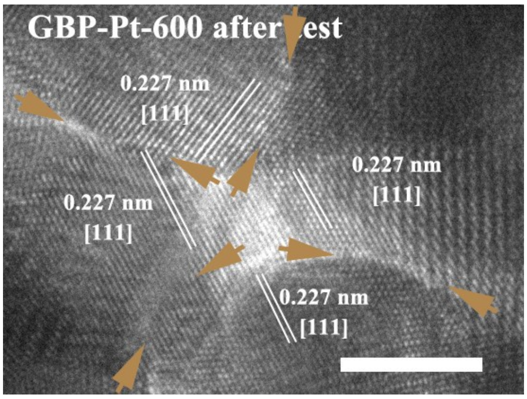

Figure S15. The HRTEM images for GBP-Pt-600 after fuel cell test.

S16. The Brunauer Emmett Teller analysis for commercial Pt.

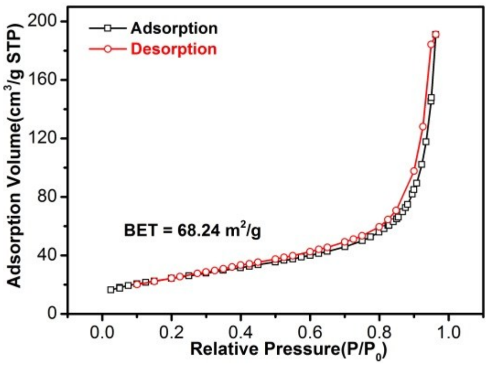

Figure S16. The Brunauer Emmett Teller analysis of commercial Pt.

S17. The durability test against the number of cycles for GBP-Pt-600.

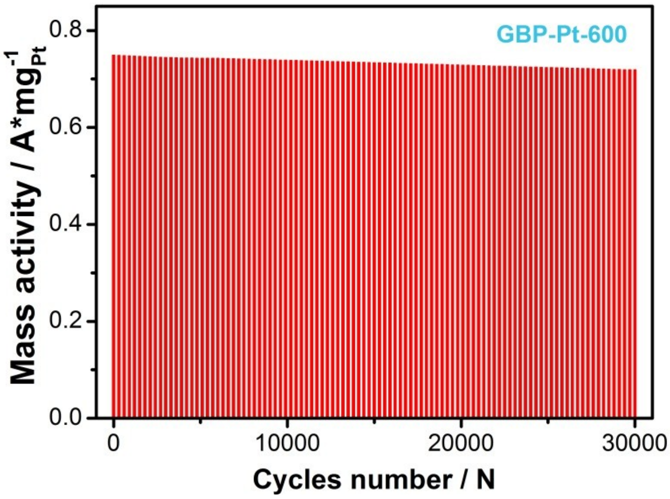

Figure S17. The durability test against the number of cycles.

S18. The TEM analysis for durability test.

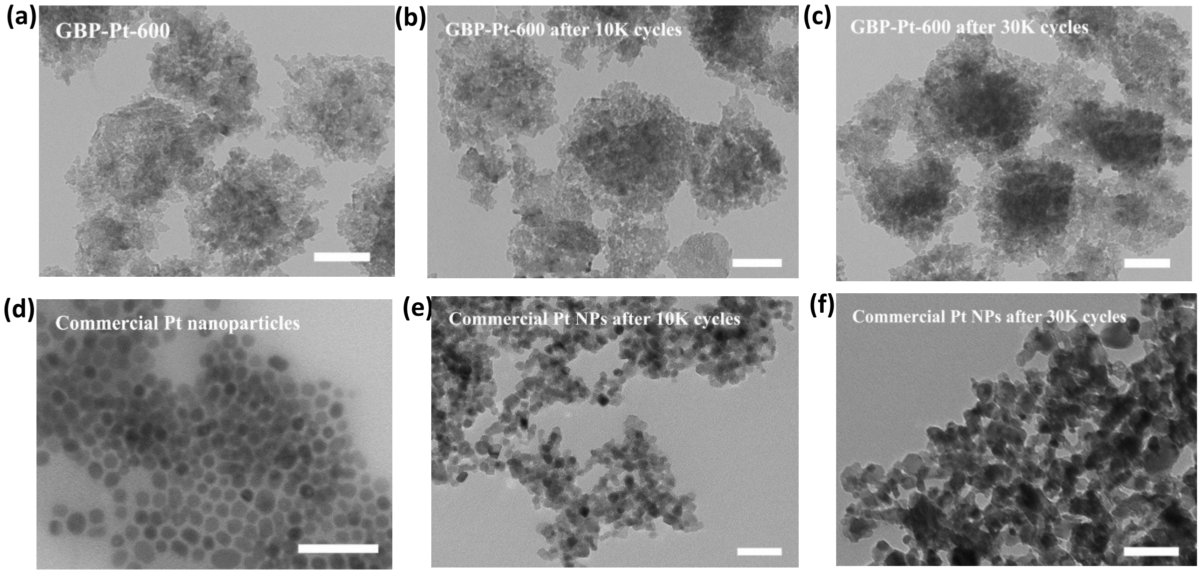

Figure S18. The corresponding TEM images of GBP-Pt-600 before (a) and after 10,000 (b) and 30000 (c) cycles of ADT, respectively. The corresponding TEM images of commercial Pt catalysts before (d) and after 10,000 (e) and 30000 (f) cycles of ADT, respectively. Scale bars is 20 nm.

S19. The CO stripping test.

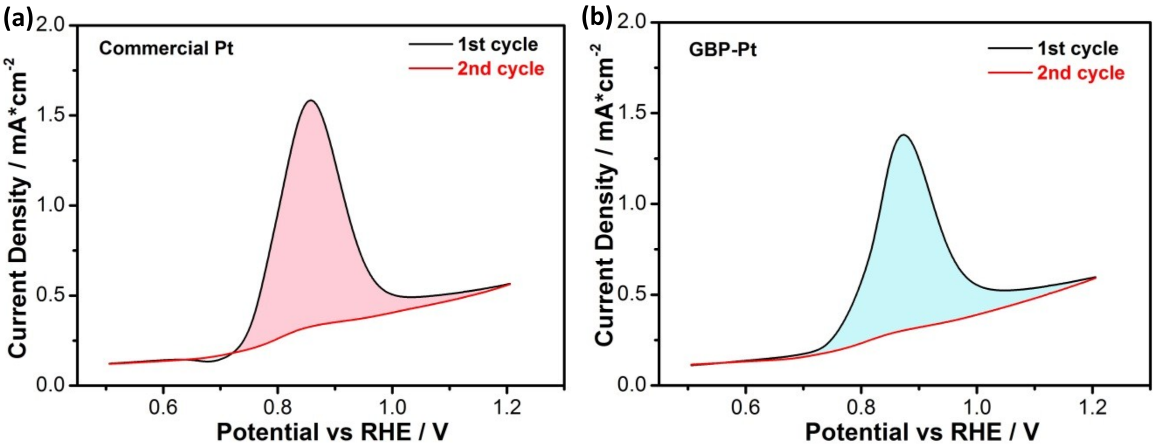

Figure S19. CO stripping voltammograms of commercial Pt (a) and GBP-Pt-600 (b) in 0.1 M $HClO_4$ solution. Scan rate: 50 mV S^{-1}; catalyst loading: 20 $\mu g_{Pt}/cm^2$.

The CO adsorption procedure in CO stripping voltammogram measurements was accomplished by polarizing the electrode at 0.2 V with CO bubbling in electrolyte solution for 10 min to adsorb monolayer CO molecules. Then, the electrode was transferred to another cell filled with Ar-saturated 0.1 M $HClO_4$ solution (without CO). Then cyclic voltammograms were conducted from 0.05 V to 1.2 V with a scan rate of 50 mV s^{-1} (*JACS.*, 2017, 139, 8152-8159. *Electrocatalysis*, 2014, 5,408–418). The theoretical charge per unit area was used as $Q_{\text{theo, Pt}} = 420\ \mu C\ cm^{-2}$ and corrected for capacitive contributions (the 2 second cycle). The calculated electrochemical surface area (ECSA) for GBP-Pt-600 is 39.3 $m^2\ g^{-1}$ and for commercial Pt is 57.7 $m^2\ g^{-1}$.

Table 1. Pt L-edge EXAFS fitting results.

samples	*Pair*	N^a	R (Å)	σ^2 ($\times 10^{-3}$Å^2)^b	E_0 *(eV)*
GBP-Pt-600	Pt-Pt	8.9 ± 0.8	2.76 ± 0.02	6.0 ± 0.6	7.4 ± 0.7
Commercial Pt	Pt-O	2.2 ± 0.3	2.05 ± 0.02	3.5 ± 0.3	3.6 ± 0.3
	Pt-Pt	6.8 ± 0.5	2.75 ± 0.02	7.5 ± 0.7	7.4 ± 0.6
Pt foil	Pt-Pt	12.0 ± 0.6	2.76 ± 0.02	4.7 ± 0.3	7.4 ± 0.5

[a] Product of S_0^2 and the coordinator number (N) in a given shell determines its FT amplitude. The $S_0^2 = 0.83$ was estimated by the fit of the Pt foil.

Table 2. Entropy (TS) , zero-point energies and Esolvation for adsorbates.

eV	ZPE	Esolvation	TS
*OH	0.330	-0.574	/
*OOH	0.427	-0.481	/
H_2(g)	0.272	/	0.405
H_2O(l)	0.575	-0.086	0.581

Table 3. The comparisons of reported Pt-based electrocatalysts.

Catalysts	Half-wave potential vs RHE (V)	Specific Activity (mA*cm^{-2})	Drop after 10000 cyeles	Ref.
GBP-Pt-600	0.941	1.67	3.4%	This work
Commerical Pt	0.883	0.25	33.2%	This work
Rh-doped Pt NWs	0.92	1.63	9.2%	*JACS.*, 2017, 139, 8152-8159.
Partially ordered fct-FePt	0.927	3.16	---	*Nano Lett.*, 2015, 15, 2468.
Pd@PtnL icosahedra	0.925	1.36	8%	*Nat. Commun.*, 2015, 6, 7594.
R-PtNWs	0.899	1.59	5.5%	*Science*, 2016, 354, 1414-1419.
Rh-doped Pt−Ni octahedral	0.927	---	12%	*Nano Lett.*, 2016, 16, 1719.
Pt_3Co-700	0.945	---	8%	*Nat. Mater.*, 2013, 12, 81.
PtCuBiMn nanosheets	0.923	2.41	3.8%	*Adv. Mater.*, 2017, 29, 1604994.